Molecular Therapy
Methods & Clinical Development
Original Article

Intrabiliary infusion of naked DNA vectors targets periportal hepatocytes in mice

Sereina Deplazes,[1] Andrea Schlegel,[2] Zhuolun Song,[2] Gabriella Allegri,[1] Nicole Rimann,[1] Tanja Scherer,[1] Melanie Willimann,[1] Lennart Opitz,[3] Sharon C. Cunningham,[4] Ian E. Alexander,[4,5] Anja Kipar,[6] Johannes Häberle,[1] Beat Thöny,[1] and Hiu Man Grisch-Chan[1]

[1]Division of Metabolism and Children's Research Center, University Children's Hospital Zürich, Steinwiesstrasse 75, 8032 Zürich, Switzerland; [2]Swiss HPB and Transplant Center, Department of Surgery, University of Zürich Hospital, Zürich, Switzerland; [3]Functional Genomics Center Zürich, University of Zürich/ETH Zürich, Zürich, Switzerland; [4]Gene Therapy Research Unit, Children's Medical Research Institute and Children's Hospital at Westmead, Faculty of Medicine and Health, The University of Sydney, Camperdown, NSW, Australia; [5]Discipline of Child and Adolescent Health, Sydney Medical School, Faculty of Medicine and Health, The University of Sydney, Westmead, NSW, Australia; [6]Laboratory for Animal Model Pathology, Institute of Veterinary Pathology, Vetsuisse Faculty University of Zürich, Zürich, Switzerland

Hydrodynamic tail vein injection (HTV) is the "gold standard" for delivering naked DNA vectors to mouse liver, thereby transfecting predominately perivenous hepatocytes. While HTV corrects metabolic liver defects such as phenylketonuria or cystathionine β-synthase deficiency, correction of *spf*^{ash} mice with ornithine transcarbamylase (OTC) deficiency was not possible despite overexpression in the liver, as the OTC enzyme is primarily expressed in periportal hepatocytes. To target periportal hepatocytes, we established hydrodynamic retrograde intrabiliary injection (HRII) in mice and optimized minicircle (MC) vector delivery using luciferase as a marker gene. HRII resulted in a transfection efficiency below 1%, 100-fold lower than HTV. While HRII induced minimal liver toxicity compared with HTV, overexpression of luciferase by both methods, but not of a natural liver-specific enzyme, elicited an immune response that led to the elimination of luciferase expression. Further testing of MC vectors delivered via HRII in *spf*^{ash} mice did not result in sufficient therapeutic efficacy and needs further optimization and/or selection of the corrected cells. This study reveals that luciferase expression is toxic for the liver. Furthermore, physical delivery of MC vectors via the bile duct has the potential to treat defects restricted to periportal hepatocytes, which opens new doors for non-viral liver-directed gene therapy.

INTRODUCTION

The liver is a target organ for the treatment of many inherited as well as acquired metabolic disorders, due to its essential role in the metabolism and detoxification. A promising approach for future treatment is gene therapy. At present, most liver-targeted gene therapy clinical trials are based on gene addition using episomal viral vectors, predominately adeno-associated viral vectors (AAV).[1,2] Despite the many advantages of AAV-mediated gene delivery, concerns regarding immunogenicity, limited DNA-packaging capacity, the risk of insertional carcinogenesis, high cost of production, and readministrations still remain.[1–8] Consequently, the development of non-viral gene therapy is re-emerging as an alternative technology because of the more favorable biosafety profile and low production costs.[9,10] The number of approved non-viral gene therapy drugs is increasing rapidly, predominated by RNA technology (for review see Kulkarni et al.[11]). Nevertheless, non-viral based delivery of naked DNA also has inherent hurdles to overcome such as poor gene delivery. Although naked DNA vectors devoid of bacterial sequences, known as minicircles (MCs),[12] or vectors free from antibiotic resistance genes,[13,14] greatly improve persistent gene expression, the effectiveness of non-viral gene transfer into the nucleus remains a major technical limitation. In the late 1990s, Liu et al.[15] and Zhang et al.[16] established an experimental approach for targeting nucleic acids to hepatocytes in rodents via so-called hydrodynamic tail vein delivery (HTV). Since high gene expression was achieved, HTV has become a popular delivery method, primarily in rodents, for nucleic acids (for review see Bonamassa et al.[17]) and even viruses for improving transduction efficiency.[18] Stable therapeutic correction of genetic mouse models for phenylketonuria (PKU)[19,20] and cystathionine β-synthase (CBS) deficiency[21] was successfully achieved by delivery of non-integrating MC vectors consisting of a liver-specific expression cassette via HTV.

Ornithine transcarbamylase (OTC) deficiency (OMIM #311250), an X-linked recessive metabolic disorder, is the most prevalent inherited defect of ureagenesis.[22] OTC (EC 2.1.3.3) is a key urea cycle enzyme in the liver, involved in the detoxification of ammonia by converting it to

Received 28 June 2022; accepted 7 October 2022;
https://doi.org/10.1016/j.omtm.2022.10.006.

Correspondence: Dr. Beat Thöny, Division of Metabolism and Children's Research Center, University Children's Hospital Zürich, Steinwiesstrasse 75, 8032 Zürich, Switzerland
E-mail: beat.thoeny@kispi.uzh.ch
Correspondence: Dr. Hiu Man Grisch-Chan, Division of Metabolism and Children's Research Center, University Children's Hospital Zürich, Steinwiesstrasse 75, 8032 Zürich, Switzerland
E-mail: hiuman.grisch@kispi.uzh.ch

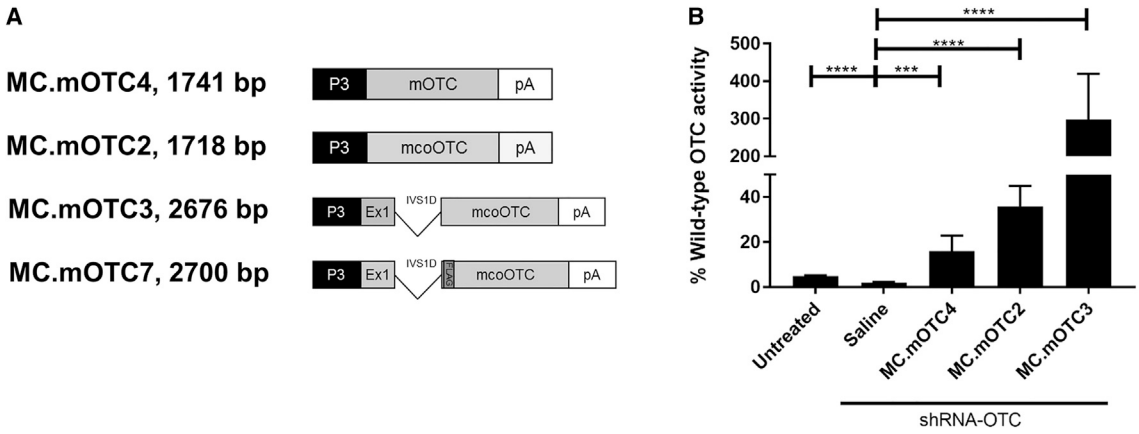

Figure 1. Optimization of MC vectors and assessment of OTC expression in *spf^{ash}* mice upon HTV infusion

(A) Schematic of the MC vectors. (B) OTC activity in liver lysate from treated *spf^{ash}* mice after HTV (n = 3–4 mice, n = 2 mice for saline group). The data presented are the average of all mice which were sacrificed when signs of neurological dysfunction were observed 4–11 days after administration of rAAV2/rh10-shRNA-OTC (at the age of 6–10 weeks old). Data were analyzed by two-way ANOVA and Sidak's multiple comparison test. ***p <0.001, ****p <0.0001.

urea for secretion. Complete deficiency of OTC function can lead to life-threatening episodes of hyperammonemia. Current conventional therapies include dietary protein restriction and use of nitrogen scavenger medication.[23,24] Orthotopic liver transplantation is the only cure but is limited by the shortage of size-matched donor livers, mortality, and morbidity.[25] Proof of concept of gene therapy has been extensively investigated in a pre-clinical model of OTC deficiency, the *spf^{ash}* mouse. Most of these studies use *in vivo* gene addition with AAV vector-based delivery, which results in long-term correction of OTC deficiency in adult mice.[26–28] A recent clinical study using AAV8-mediated gene transfer of human OTC in late-onset adult OTC patients has shown partial responses at high doses of 2×10^{12} to 1×10^{13} vector genome (vg)/kg.[29] Nevertheless, the death of patients receiving very high doses (>5×10^{13} vg/kg) of AAV vectors in clinical trials because of immunotoxicity adds to emerging safety concerns.[30,31]

OTC is predominantly expressed in hepatic periportal regions owing to liver metabolic zonation, a phenomenon that separates various metabolic pathways along the porto-central axis of the liver lobule into the periportal zone 1 including the portal triad, a transitional zone 2, and a pericentral zone 3.[32,33] Targeting OTC-expressing MC vectors to periportal hepatocytes is challenging, as it requires administration through vessels connected directly to the portal triad. Portal vein injection using hydrodynamic pressure can result in high mortality rate in rodents[34] (see also results). An alternative and potentially safer intervention compared with portal vein infusion is through the biliary system. Hydrodynamic retrograde intrabiliary injection (HRII) provides direct access to hepatocytes in the liver parenchyma through bile canaliculi and avoids first contact with Kupffer cells, which might lead to reduction in gene delivery efficiency through the portal vein.[35,36] Additionally, evidence has shown that bile may contain lower concentrations of nucleases compared with blood serum.[37] For these reasons, non-viral gene delivery of naked DNA vectors or vector DNA complexes with liposomes or nanoparticles through the biliary tract has been extensively investigated in rodent models,[38–43] dogs,[38] and pigs.[44–47] This application has also been applied to the administration of viral vectors for liver-targeted delivery in rodents and large animals.[48–53] However, non-viral gene delivery via intrabiliary injection has so far not been shown to treat any liver-defected murine models.

In this study, we aimed to establish a physical delivery of MC vectors via the bile duct to potentially correct OTC deficiency, which is primarily located at periportal hepatocytes. The gene delivery efficiency, as well as toxicity and damage to the liver of MC vectors administered through the biliary tree, were characterized in comparison with HTV. While this approach to non-viral liver targeting has the potential to specifically target periportal hepatocytes, further optimization is required to correct OTC deficiency.

RESULTS

HTV delivery of naked DNA vectors results in high OTC expression in liver but cannot correct *spf^{ash}* mice

HTV is an efficient delivery method to target naked DNA vectors to hepatocytes with a transfection efficiency of up to 18% of liver cells (see also below). Although the complete ureagenesis cycle is strictly limited to periportal hepatocytes, we first sought to deliver therapeutic vectors to treat OTC deficiency via HTV to *spf^{ash}* mice. As depicted in Figure 1A, we prepared a series of MC vectors harboring the liver-specific promoter P3 that expressed the normal murine *Otc*-cDNA (MC.mOTC4) or a codon-optimized version with (MC.mOTC3) or without (MC.mOTC2) a 5′ truncated intron 1 (IVS1D). Furthermore, vector MC.mOTC7 contains a FLAG-tagged OTC for immunohistochemical localization of the expressed OTC transgene in the liver. Note that expression and correct processing of the FLAG-tagged recombinant OTC was validated in a separate set of experiments with *spf^{ash}* mice and included insertion of the FLAG coding sequence in

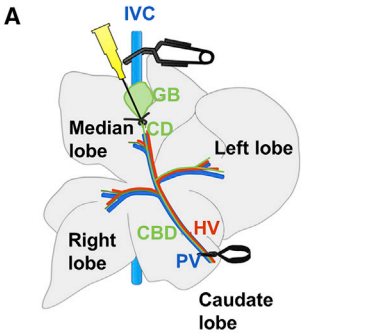

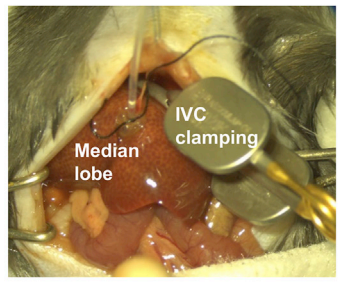

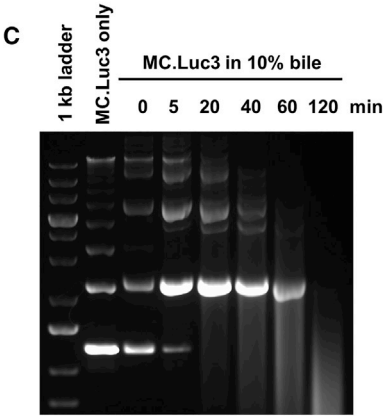

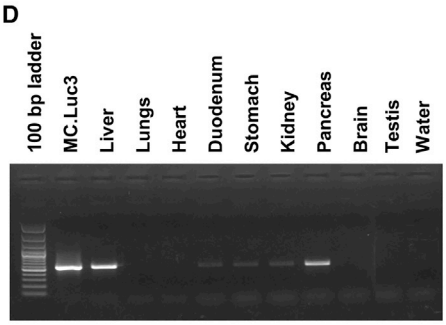

Figure 2. Outline of HRII and evaluation of vector DNA stability and biodistribution

(A) Schematic and (B) photograph of hepatobiliary anatomy and preparation for intrabiliary infusion. (C) Effect of bile acid on MC vector DNA degradation. A solution of 10% bile acid (diluted in PBS) was incubated with 1 μg of MC.Luc3 for various durations before separating on 0.8% agarose gel by electrophoresis. (D) Biodistribution of MC vectors 2 days following HRII, detected by saturated PCR. GB, gallbladder; CD, cystic duct; PV, portal vein; HA, hepatic artery; CBD, common bile duct; IVC, inferior vena cava.

exon 2, which is downstream of the mitochondrial import signal and peptidase cleavage sites (Figures S1A–S1D).

Equimolar amounts (2.9×10^{13} copies of the vector) of MC.mOTC4, MC.mOTC2, or MC.mOTC3 were infused into *spf*^{ash} mice each by HTV. Treatment efficacy was assessed by short hairpin RNA (shRNA)-mediated knockdown of residual endogenous OTC expression, which leads to induction of severe hyperammonemia in untreated mutant mice. To this end, 1 day following infusion, rAAV2/rh10 encoding an shRNA-OTC to specifically knock down genomic m*Otc*-mRNA expression was administered intraperitoneally. All HTV/MC vector-treated mice showed thereafter signs of severe ataxia due to hyperammonemia (Figure S2) and had to be euthanized within 4–11 days post shRNA infusion. OTC enzyme activity in whole liver extracts was determined in all sacrificed mice (Figure 1B). Infusion of MC.mOTC3 gave rise to the highest liver OTC activity (298% of normal), and mice treated with MC.mOTC4 and MC.mOTC2 had OTC activity levels equivalent to 16% and 36% of levels in wild-type mice, respectively.

Despite the exceedingly high enzymatic OTC activity, mice still suffered from hyperammonemia following the knockdown of residual OTC. To investigate in depth, MC.mOTC7 vectors were infused into the mouse livers via HTV and the livers were collected for immunohistochemical staining for FLAG-tagged OTC protein. Here, we identified that although there were almost 10% positively transfected hepatocytes, positive cells were clustered around the central vein (zone 3; Figure S1D), which explained the lack of treatment efficacy.

Open surgery for portal vein infusion results in high mortality

To deliver MC vectors directly to hepatocytes located in periportal areas (zone 1), we first sought to access the liver lobules via intraportal injection. We therefore adopted the method described by Budker and colleagues,[34] but made the minor modification of clamping the suprahepatic vena cava before, instead of after, injection to increase the intraportal hydrostatic pressure. Following hydrodynamic portal vein injection, approximately 63% (15/24) of the OTC-deficient *spf*^{ash} mice did not survive the procedure due to excessive bleeding, while the mortality rate for wild-type C57Bl/6J mice was 20% (1/5). We did not further analyze the cause of lethality; however, the high number of deaths among OTC-deficient mice has been previously observed by others and is most likely attributable to hepatopathy attributable to the underlying metabolic disorder.[54]

Retrograde intrabiliary injection results in normal survival

Next, we evaluated access via the biliary tree as a potential alternative to portal vein injection. We first established the surgical procedure, which was termed "hydrodynamic retrograde intrabiliary injection," HRII (for surgical details see materials and methods and Figures 2A and 2B). Retrograde infusion of 1 mL of saline solution within 30 s (flow rate of 33 μL/s, see Zhang et al.[38]) resulted in rupture of the gallbladder in 45% (9/19) of the injected mice. When the volume was reduced to 0.8 mL and the infusion time shortened to 10 s (flow rate of 80 μL/s), no leakage was found. Using those parameters, we subjected over 100 mice to the HRII procedure, which includes open surgery and biliary infusion, without any further losses and, thus, an overall survival rate close to 100%.

Degradation of MC vector in bile acid is not a critical factor, and infusion via the bile duct results primarily in liver cell transfection

Bile acid has been reported to cause DNA strand breaks.[55] As the murine biliary tree is filled with 24–48 μL (1 μL/g of an animal; total 480–960 μL of bile in a 20-g mouse) of bile acid[56,57] and the injection

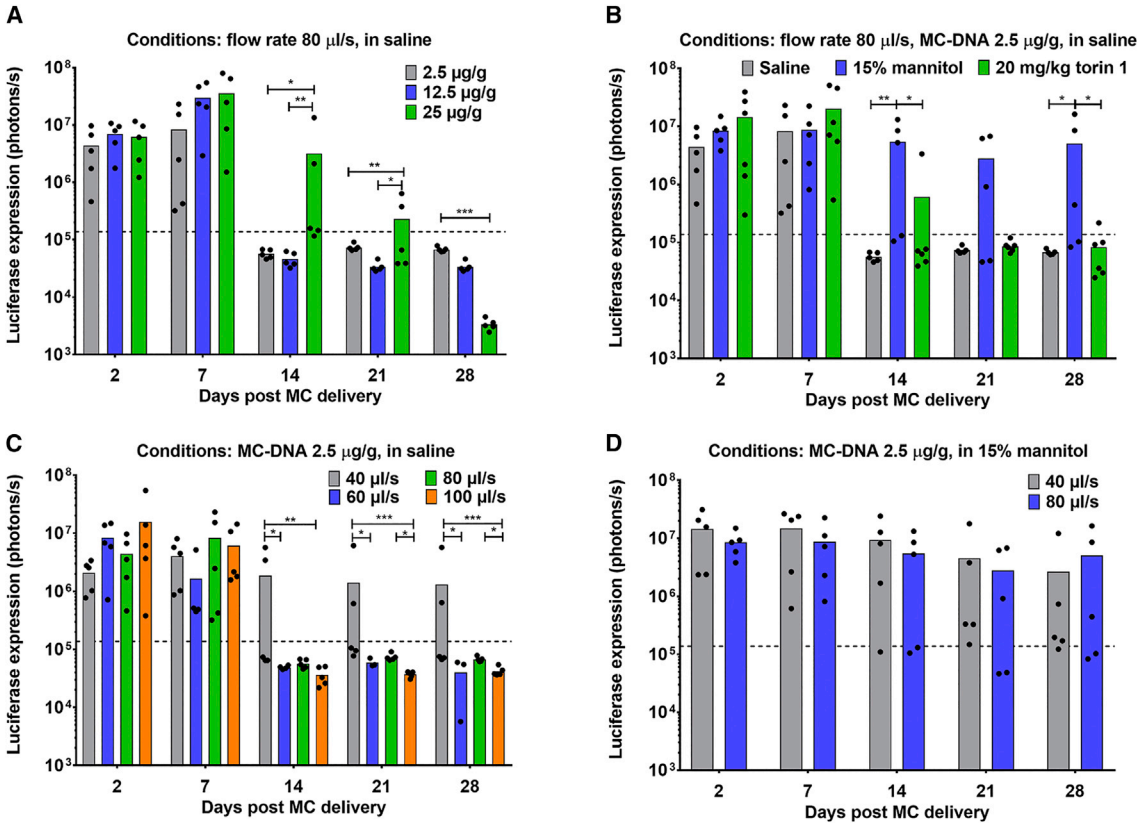

Figure 3. Optimizing conditions for HRII into mice by following luciferase expression in the liver

Hepatic luciferase expression (photons per second) was analyzed in mice by *in vivo* bioimaging system (IVIS) following HRII using different injection parameters: (A) vector dose; (B) additives; (C) flow rates; (D) pressure plus mannitol. Results are expressed as the mean of 5–6 mice with one exception of three mice in the group with a flow rate of 60 µL/s on days 14, 21, and 28 (C; due to unexpected deaths of two mice not related to surgical intervention and infusion). Each dot in the columns represents an individual mouse. The data from (A)–(C) were analyzed by the Kruskal-Wallis test, followed by Dunn's post hoc test for multiple comparisons. The data from (D) were analyzed by the Mann-Whitney U test. $^{*}p < 0.05$, $^{**}p < 0.01$, $^{***}p < 0.001$. The results were not statistically significant where no p value is shown. Note that data from mice treated with 2.5 µg/g DNA in 15% mannitol with the flow rate of 80 µL/s are shown in (C) and (D) for a comparison. The dotted line represents the background level of luciferase expression (1.4×10^5 photons/s) which was determined with five mice that received no MC vectors.

volume is between 0.4 and 0.8 mL, we expected the bile acid to be diluted down to 2.5%–5% of the original concentration upon HRII. To test the stability of MC in bile, MC vectors were incubated with a bile-acid-containing solution (10% bile acid in PBS [v/v]) at 37°C for up to 120 min. Degradation of MC vector was apparent after 20 min while complete DNA degradation was observed after 120 min (Figure 2C). Since the injection time of HRII is 10 s and the bile acid is diluted 2–4 times compared with the experiment above, we concluded that degradation of the MC vector is likely not a critical factor. Next, we performed endpoint PCR to detect MC vector in various tissues 2 days following HRII. We found a strong positive signal for a band indicating MC vectors within liver tissue, weaker bands for pancreas, kidney, stomach, and duodenum, and no signal for the other organs tested (Figure 2D).

Optimization of HRII for liver gene expression

To determine the best delivery conditions for transfection of MC vectors into liver cells via HRII, we optimized various parameters, including vector dose, additives, flow rates, and pressure (for detailed description see materials and methods). These studies were performed in wild-type mice using the MC.Luc3 vector that expresses luciferase via the liver-specific promoter P3. We followed luciferase activity in the liver for 28 days post injection by an *in vivo* bioimaging system (IVIS). The results are presented in Figure 3 as the liver-specific expression of luciferase *in vivo* at each time point (Figure S3). The default infusion condition is set to be a flow rate of 80 µL/s (0.8 mL in 10 s in a saline solution containing 2.5 µg DNA/g per mouse). The data from mice treated with the default infusion condition are shown in Figures 3A–3C for comparison.

First, luciferase expression was compared in mice with different doses of MC vectors, i.e., 2.5 µg, 12.5 µg, and 25 µg DNA/g of mouse (flow rate of 80 µL/s, Figure 3A). On days 2 and 7 post delivery, all treatment groups exhibited similar luciferase activity. Thereafter, expression dropped below background level by day 28 in all treatment groups. As higher vector concentrations did not improve persistent

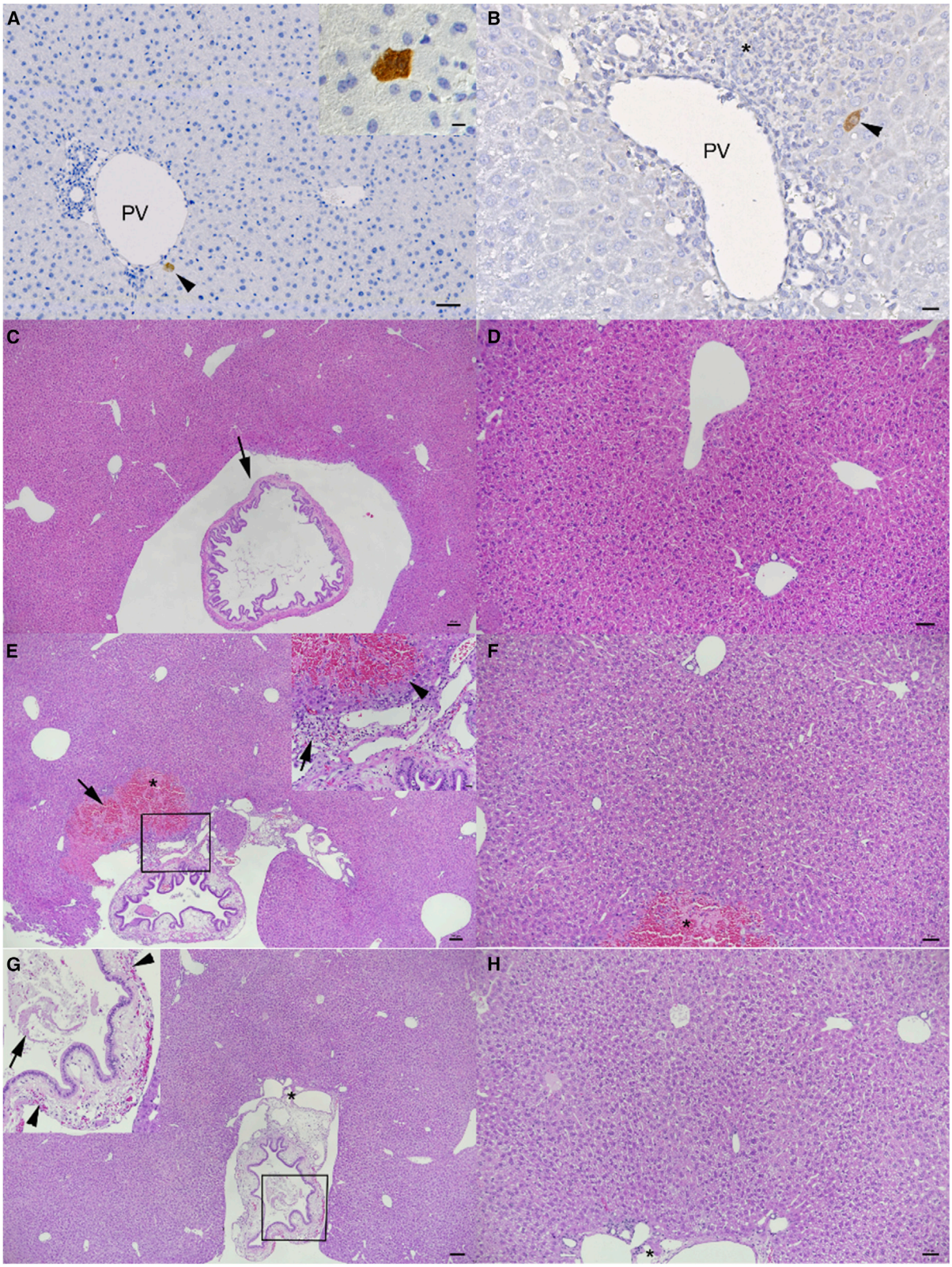

(legend on next page)

luciferase expression beyond day 28, a vector dose of 2.5 μg/g, equivalent to 50 μg for a 20-g mouse, was used for all subsequent experiments. Next, we optimized two additional parameters, including different additives (15% mannitol or pre-treatment with 20 mg/kg autophagy inducer torin 1), and a series of different flow rates (40 μL/s, 60 μL/s or 100 μL/s in saline solution). Long-term luciferase expression was achieved in mice that received MC vectors in 15% mannitol injection solution, but not pre-treated with torin 1 (Figure 3B) or with the flow rate of 40 μL/s (Figure 3C). From this observation, we concluded that a hypertonic solution with 15% mannitol and at a lower flow rate of 40 μL/s is beneficial for continuous transgene expression. Finally, we tested whether luciferase expression could be further increased or prolonged by injection of 2.5 μg/g vector in 15% mannitol in combination with "low-pressure" (40 μL/s) compared with "high-pressure" (80 μL/s) infusion (Figure 3D). Here we found no significant differences between the treatment groups. Taken together, we found that the "low-pressure" injection of a volume of 0.4 mL 15% mannitol in 10 s, i.e., a flow rate of 40 μL/s, resulted in the best conditions for hepatic luciferase expression upon delivering MC vectors via HRII. We thus applied these conditions in all subsequent experiments. Interestingly, a common phenomenon was observed in all treatment groups (Figures 3A–3D), namely that high luciferase expression was eliminated in individual mice beyond day 14. As will be shown below, we found that this sudden loss of gene expression was due to liver cell toxicity caused by high-level luciferase expression.

Mice from each treatment group were sacrificed at day 30 and their livers analyzed for vector copy numbers and luciferase-positive cells. As summarized in Table S1, we found in all samples between 0.04 and 0.70 vector copy numbers per diploid genome, concomitant with 0.07%–0.20% of luciferase-positive cells. These results do not consistently reproduce what was observed in the IVIS analyses at day 28 (Figure 3) but reflect the loss of luciferase expression and/or MC.Luc3. An example for immunohistochemical staining for luciferase 30 days post HRII is illustrated in Figure 4A (flow rate of 40 μL/s) and Figure 4B (flow rate of 80 μL/s) where rare positive hepatocytes were observed, occasionally confirmed to be located in periportal areas, i.e., zone 1–2.

Histological evaluation of mouse liver following HRII

Hydrodynamic injection via the bile duct concomitant with blockage of inflow and outflow of the liver resulted in transient swelling, paleness, and firm consistency after administration (Figure 2B). To better characterize the effects of HRII on the liver, we performed a histological analysis 2 days following administration of saline. While control mice did not exhibit any histological changes (Figures 4C and 4D), livers of mice that had undergone HRII with a flow rate of 40 μL/s showed focal areas of coagulative necrosis in the parenchyma surrounding the gallbladder (Figures 4E and 4F). These were generally larger and more numerous in animals that had received the larger volume of 0.8 mL (flow rate of 80 μL/s). These animals also exhibited acute focal hemorrhage into the gallbladder, in the gallbladder wall, and in the surrounding tissue (Figures 4G and 4H). There were occasional focal areas of mononuclear infiltration around the site of ligation of the cystic duct and stretching from these. Otherwise, the liver parenchyma was unaltered, as in control mice.

Elimination of luciferase after high-level gene expression in mouse liver

The loss of luciferase upon HRII or HTV injection of MC.Luc3 due to the potential toxicity induced by robust expression in liver tissue was analyzed in more detail. We have previously reported that transgenic expression of endogenous (murine) phenylalanine hydroxylase (m*Pah*) for liver gene therapy of PKU mice using a comparable MC vector infused by HTV did not elicit any immune-stimulatory response.[20] For better quantification, we performed a side-by-side comparison in wild-type mice by infusing MC.PKU37 expressing a FLAG-tagged mouse PAH[19,20] or MC.Luc3 (expressing the luciferase) via HTV with both vectors containing the P3 promoter. At days 2 and 7 post infusion, the number of transfected cells were not significantly different for both vectors and transgenes (Figures 5A–5D and 5G), i.e., between 12% and 18% (and mainly located at the perivenous area). By day 21, expression from MC.Luc3 dropped to 0.3% but remained unchanged for MC.PKU37 (Figures 5E–5G).

Next, we quantified luciferase enzyme activity for MC.Luc3-treated mice and vector copy numbers for both vectors at all three time points. For comparison, we included mice treated by HRII with MC.Luc3 (2.5 μg/g plus 15% mannitol, flow rate 40 μL/s; see Figure 3D). Luciferase expression dropped post HTV from 15,557 ± 3,281 RLU/μg on day 2 post infusion to 26 ± 16 RLU/μg on day 21, a 600-fold reduction (Figure 6A). A similar dramatic loss was observed for vector copy numbers for MC.Luc3 but not MC.PKU37 (Figure 6B). The liver damage markers aspartate transaminase (AST) and alanine transaminase (ALT) were transiently elevated at day 2 post infusion for HTV but not HRII, with the highest levels in the presence of MC.Luc3 (Figures 6C and 6D). This hints toward liver toxicity upon HTV, but not HRII, and is exacerbated with luciferase expression. Production of interleukin-6 (IL-6), a pro-inflammatory cytokine, was analyzed in plasma on day 2 after gene delivery. Our data revealed that luciferase expression (MC.Luc3) upon HRII

Figure 4. Transfected hepatocytes and morphological features in livers 2 days after HRII

(A and B) Luciferase expression in hepatocytes (arrowheads) after delivery of 2.5 μg/g MC.Luc3 in 15% mannitol with a flow rate of 40 μL/s (A) or 80 μL/s (B). PV, portal vein; asterisk indicates focal periportal mononuclear infiltration. (C and D) Unaltered liver of untreated control mouse (arrow points to gallbladder). (E and F) Liver after saline infusion at 40 μL/s. Focal parenchymal coagulative necrosis (arrow and asterisk) adjacent to gallbladder. Inset: coagulative necrosis of hepatocytes (arrowhead) and mild leukocyte infiltration around gallbladder (arrow). Unaltered parenchyma distant from gallbladder (F). (G and H) Liver after saline infusion at 80 μL/s. (G) Fibrin and erythrocytes within gallbladder (arrow), mild hemorrhages in and around gallbladder wall (arrowheads). (H) Unaltered parenchyma close to gallbladder (asterisk, also in G). Immunohistochemistry in (A) and (B), H&E stain in (C)–(H). Scale bars, 100 μm (C, E), 50 μm (A, D, F), 20 μm (B), and 10 μm (inset A).

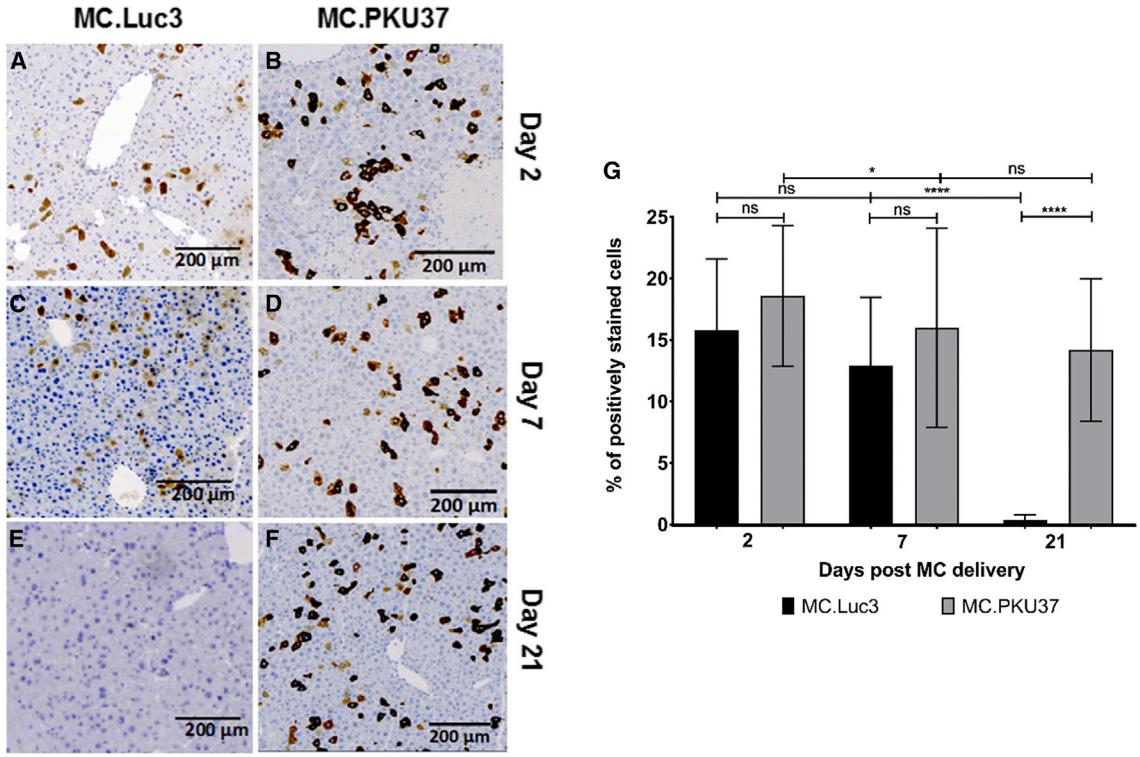

Figure 5. Comparison of luciferase and murine phenylalanine hydroxylase (m*Pah*) transgene expression in mouse liver at different time points following HTV

Mice were infused with either MC.Luc3 expressing luciferase or MC.PKU37 expressing an N-terminal FLAG-tagged PAH by HTV. Livers were harvested on day 2 (A and B), day 7 (C and D), and day 21 (E and F) for immunohistochemistry staining. (G) Quantification of immunohistochemistry staining shown in (A)–(F) by depicting the percentage of positively stained cells. Results are depicted as mean ± SD of five mice. Data were analyzed by two-tailed unpaired t test. *p <0.05, ****p <0.0001, n.s. not-significant.

or HTV and in comparison with PAH expression (MC.PKU37) or saline as control induced the strongest immune response in mice (Figure S4). We also analyzed the cell proliferation marker Ki-67 that was significantly elevated (up to 5-fold) after HTV infusion, but not HRII, and more pronounced in the presence of the luciferase-expressing vector independent of the infusion procedure (Figure 7).

Thus, while HRII induced less toxicity and liver damage than HTV, delivery of luciferase by either method, but not of, e.g., (endogenous) *Pah* as a transgene, elicited an immune response that led to the elimination of hepatic luciferase expression beyond 7 days post infusion.

RNA-sequencing transcriptome profiling in liver tissue reveals a milder immune response upon HRII compared with HTV and toxicity against luciferase overexpression

To further investigate the impact of HRII versus HTV treatment and the effect of MC vectors that express luciferase in the liver, we performed untargeted transcriptome profiling of mice treated by HRII or HTV in comparison with uninjected control mice. RNA sequencing on day 2 post infusion identified a total of 960 differentially expressed genes (DEGs) with statistical significance (false discovery rate <0.05 and $\log_2$(fold change) >0.5) in HRII-treated livers where 551 genes were upregulated and 409 genes were downregulated. In comparison, HTV-treated livers had 1,888 DEGs with 1,077 genes upregulated and 811 genes downregulated (Figures S5A–S5D). For a complete gene ontology (GO) list of biological processes (BP), see Tables S2 and S3. Overall, the immune system, including the innate immune response, was among the most significantly enriched GO-BP categories. The corresponding heatmap supports also visually the more severe impact or damage of the HTV procedure compared with HRII (Figure S5E). Although we do not have transcriptome profiling data for direct comparison with a natural liver transgene, the strong expression of luciferase might exacerbate this effect upon HTV injection. Taken together, these results indicated the likelihood of an immune response bringing about the loss of luciferase expression when there was sustained or high-level expression after hydrodynamic injection via bile duct or tail vein.

Low efficacy for correction of OTC deficiency upon delivery of therapeutic naked DNA vectors via HRII

Next, we tested whether MC vector gene delivery via HRII (flow rate of 40 µL/s, 0.4 mL of volume with 15% mannitol in 10 s), previously found to preferentially target periportal hepatocytes (Figure 4A), could correct urea cycle function. Ten adult *spf*^{ash} male mice were injected with 420 µg of MC.mOTC3, and ureagenesis was monitored pre-treatment and on days 10 and 84 following treatment using a stable isotope method with [^{15}N]ammonium chloride as tracer.[58] We found that three mice from this cohort (mice #112, #114, and #130)

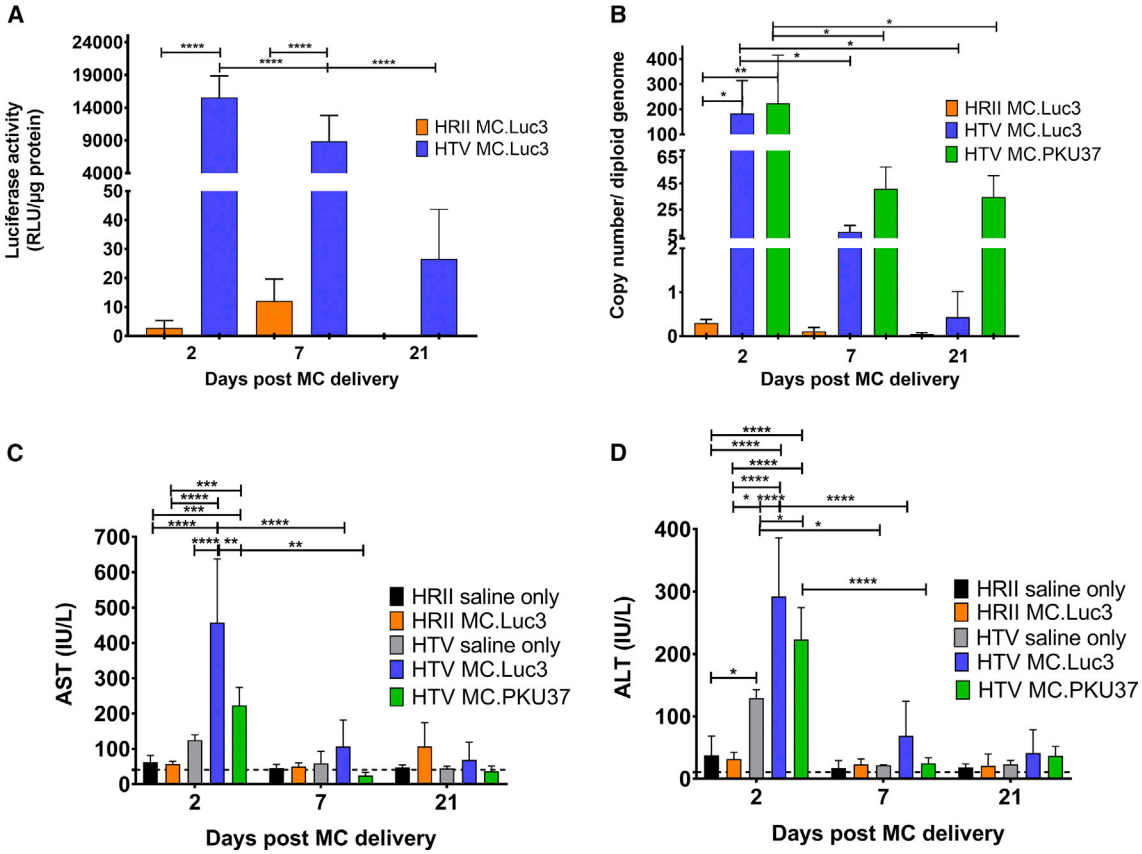

Figure 6. HRII is less efficient for gene delivery but induces less liver toxicity compared with HTV

The amount of 2.5 µg/g of MC.Luc3 or MC.PKU37 was infused into mouse liver by way of HRII or HTV. (A) Specific luciferase activity and (B) vector copy number per diploid genome upon HTV compared with HRII. (C and D) Assessment of hepatic toxicity by determining plasma aspartate aminotransferase (AST) and alanine aminotransferase (ALT). Dotted lines in graphs represent normal levels of AST and ALT in untreated mice. Data were analyzed by two-way ANOVA followed by Tukey's post hoc test for multiple comparisons. Results are depicted as mean ± SD of five mice except for the group that received saline only via HTV (n = 3). Significance is indicated where applicable. $^{*}p$ <0.05, $^{**}p$ <0.01, $^{***}p$ <0.001, $^{****}p$ <0.0001.

showed sustained and significant augmentation of ureagenesis enrichment shifted above threshold,[58] i.e., in the range of wild-type mice (Figure 8A). Next, we delivered rAAV2/rh10-shRNA-OTC to mice #112 and #114 to knock down the expression of endogenous m*Otc*-mRNA and tested for treatment efficacy by induction of hyperammonemia (note that owing to the highest severity grade of this assay, the Swiss Law of Animal Protection allowed only a limited number of mice to be tested). Figure 8B shows the percentage of [^{15}N]urea enrichment upon shRNA-OTC treatment. Here, the wild-type mouse (#85) reduced [^{15}N]urea enrichment following shRNA-OTC treatment, as expected,[59] but did not show dramatic weight loss (Figure 8C) nor very high plasma ammonia levels (Figure 8D). By contrast, the saline-treated *spf^{ash}* mouse (#67) and one MC.mOTC3-treated *spf^{ash}* mouse (#112) had to be euthanized on day 13 upon the development of dramatic weight loss and hyperammonemia, while the other MC.mOTC3-treated *spf^{ash}* mouse (#114) retained normal body weight and ammonia levels, consistent with their [^{15}N]urea enrichment (Figures 8A and 8B), confirming the successfully corrected periportal hepatocytes upon intrabiliary infusion.

In conclusion, while MC vectors expressing OTC delivered via HTV were highly efficient in transducing (mainly perivenous or zone 3) hepatocytes, correction of OTC deficiency and rescue for survival upon HRII could only be observed with limited efficacy. This study proves that physical delivery of MC vectors via the bile duct has the potential to treat OTC deficiency in periportal hepatocytes, although the HRII method still needs optimization (see discussion).

DISCUSSION

This study demonstrates that gene delivery using naked DNA vectors (MCs) via the bile duct to target periportal hepatocytes results in low but sustained gene expression. The optimal HRII condition was set to a volume of 0.4 mL 15% mannitol in 10 s (flow rate of 40 µL/s, Figure 3). Although the transfection rate (<1%) and the vector copy number were relatively low, the transfected hepatocytes were mainly located in the periportal area (Figures 4A and 4B). We observed mild coagulative necrosis in the parenchyma surrounding the gallbladder and near the ligation site at the cystic duct on day 2 (Figures 4E–4H), yet there was no elevation of serum liver enzymes (AST and

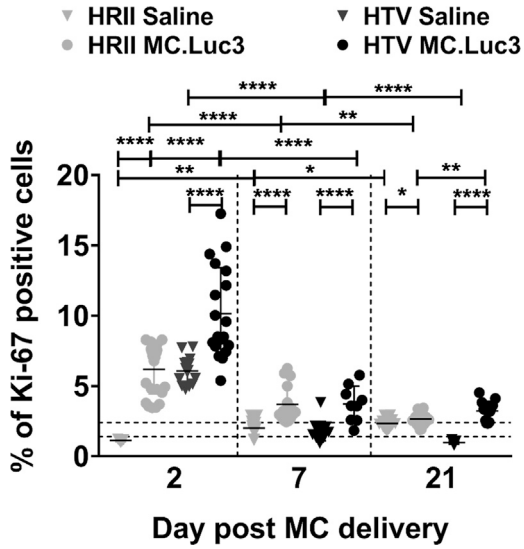

Figure 7. Test for Ki-67 proliferation marker upon HRII or HTV infusion of MC.Luc3 compared with saline control

Mice were treated by HRII or HTV infusion of saline or MC.Luc3 (n = 5 for each group) and sacrificed at different time points. The different liver lobes were quantified by immunohistochemistry staining for Ki-67 positive cells. The dotted lines mark the range between the 10th and 90th percentile determined by two untreated wild-type mice. The dot plot indicates mean with SD; symbols mark individual lobes of the five mice. Statistics: two-sided unpaired t test. *p <0.05, **p <0.01, ****p <0.0001, n.s. p >0.05.

ALT; Figures 6C and 6D) upon pressurized injections of saline or hypertonic solution. In addition, all mice survived the surgical treatment (>100 mice). We thus concluded that the surgical procedure for the intrabiliary injection route is a safer and a less invasive delivery method compared with portal vein injection for targeting periportal hepatocytes. In parallel, we have recently reported that HRII of MC vectors applies to larger animal models such as domestic small pigs, where we found a stable hepatocyte transfection and no acute adverse complications.[47] A further improvement toward mitigating the invasiveness of the procedure for infusion via the bile system could be endoscopic retrograde cholangiopancreatography (ERCP) that was reported for delivering plasmid DNA to adult pigs.[44]

Firefly luciferase is a widely used imaging reporter transgene that allows visualization of luciferase expression in real-time bioluminescence imaging of mice.[60] Infusion of MC vectors expressing luciferase (MC.Luc3) via bile duct or tail vein yielded high initial luciferase expression but was reduced or eliminated 7 days later. A similar phenomenon was also reported by others when a threshold of luciferase expression was reached.[61] This effect was only observed with luciferase as transgene but not with an endogenous hepatic (therapeutic) transgene such as m*Pah* (MC.PKU37), where the number of transfected hepatocytes remained persistent in HTV-treated mice (Figures 5 and 6). Furthermore, we have previously reported life-long correction in PKU and CBS deficiency in mice after targeting MC vectors consisting of therapeutic transgenes to the livers upon a single dose of HTV.[19–21] The clearance of luciferase expression was due to innate or antigen-dependent immune responses triggered by the foreign protein (Figures 5, 6, S4, and S5). These results were confirmed by others showing that CD8 T cell epitopes provoked a robust immune response in immunocompetent mice but not in immunocompromised mice after exposure to luciferase protein.[61–64] Up to now, the immune response against luciferase in other organs has not been reported.

Finally, our study attempted to determine whether hydrodynamic retrograde intrabiliary-delivered MC vectors correct OTC deficiency in *spf*^{ash} mice, since urea cycle function is primarily active in the periportal regions of the hepatic lobules. To improve the efficacy of the therapeutic OTC-expressing vector, we first optimized the expression cassette in the MC constructs. MC.mOTC3 was designed, based on our previous experience,[19] to contain a codon-optimized m*Otc* combined with a truncated IVIS1D and resulted in much higher OTC activity in HTV-treated mouse livers compared with MC.mOTC4 or MC.mOTC2 (Figure 1B). However, the HTV approach that targets primarily perivenous hepatocytes could not prevent the *spf*^{ash} mice from developing hyperammonemia (Figure S2) following knockdown of residual endogenous m*Otc*-mRNA, despite reaching up to 300% wild-type enzyme activity, thus highlighting the importance of targeting periportal hepatocytes. In contrast, partial restoration of ureagenesis function was achieved in the *spf*^{ash} mouse when MC.mOTC3 was delivered through the bile duct (Figure 8). We speculated that the low cell transfection efficiency at the periportal region upon HRII was an obvious explanation for the limited efficacy to treat OTC-deficient mice. To overcome this problem in future experiments, we propose to take advantage of a selective growth advantage of, for instance, the corrected hepatocytes.[65–67] In this context it is important to note that we used episomal-based naked DNA vectors for liver-targeted gene therapy; hence, the vectors might be lost in gene-corrected hepatocytes that undergo cell proliferation unless they contain elements with the potential for autonomous replication.[68]

In summary, we found that delivery through the biliary tree is feasible and safe and has the potential for injection or reinjection of non-viral naked DNA vectors in (pediatric) patients, even through less invasive ERCP-mediated hydrodynamic delivery or percutaneous transhepatic cholangiography as an alternative. Moreover, by combining a novel class of autonomously replicating non-viral naked DNA vector and *in vivo* selection, the intrabiliary delivery method may have a great impact on the treatment of genetic (metabolic) liver defects.

MATERIALS AND METHODS

Animal husbandry, genotyping, and AAV treatment

The State Veterinary Office of Zürich approved all animal experiments; experiments were carried out according to the guidelines of the Swiss Law of Animal Protection (licenses ZH130-2014 and ZH072-2017), the Swiss Federal Act on Animal Protection (1978), and the Swiss Animal Protection Ordinance (1981). Wild-type C57BL/6JRccHsd female or male mice aged 6–8 weeks were obtained from Envigo (Horst, the Netherlands). For therapeutic correction

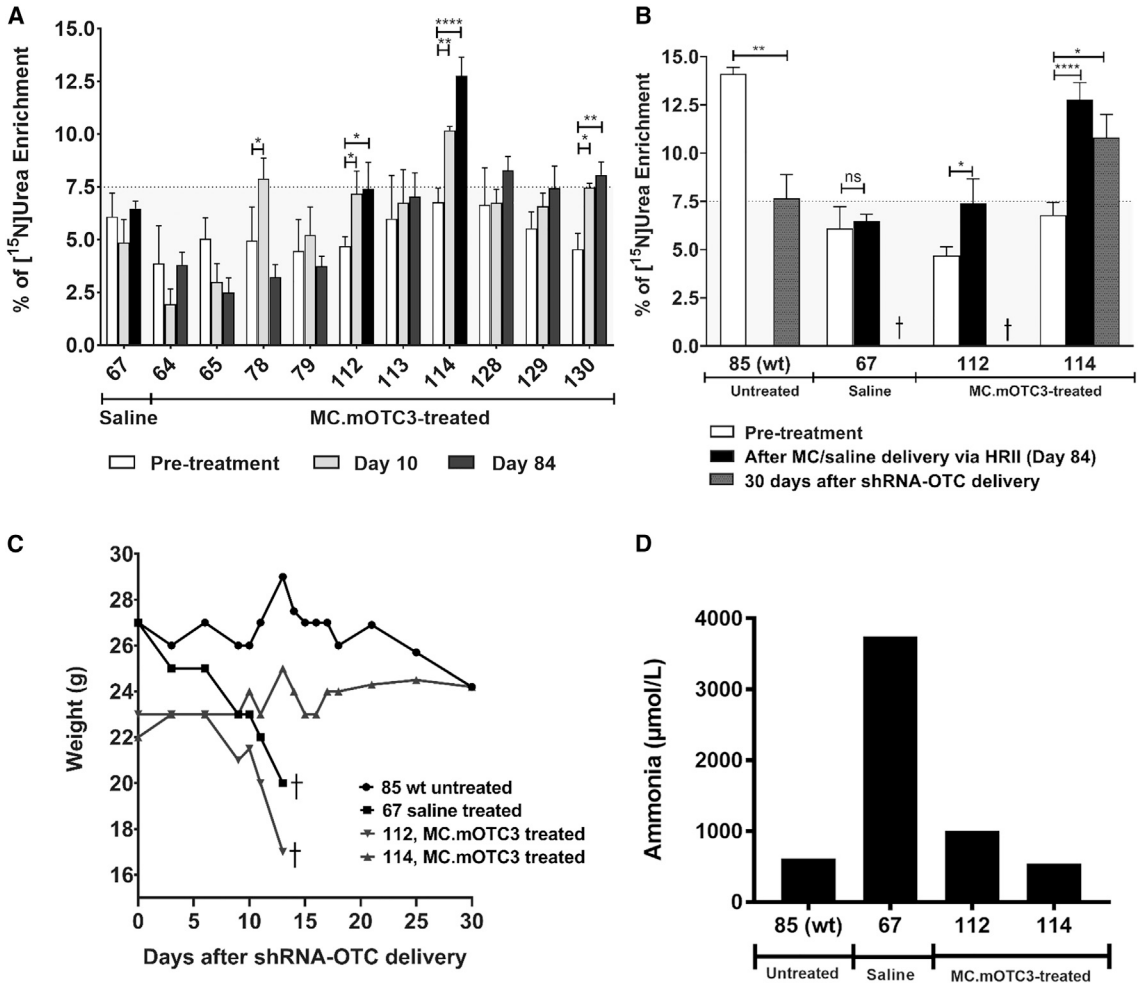

Figure 8. Correction of OTC deficiency and rescue for survival were observed upon HRII

Ureagenesis assay at different time points of the entire cohort (A) after HRII and (B) after administration of rAAV2/rh10-shRNA-OTC. Data were analyzed by two-way ANOVA. Sidak's multiple comparison test. (C) Weight of each mouse after delivery of rAAV2/rh10-shRNA-OTC. WT, wild-type mouse; dagger indicates mice euthanized due to health issues 13 days after administration of rAAV2/rh10-shRNA-OTC (at the age of 19–22 weeks old). (D) Blood ammonia level measurement upon sacrifice. $^{*}p$ <0.05, $^{**}p$ <0.01, $^{****}p$ <0.0001, n.s. not significant.

studies, we used hemizygous OTC-deficient *spf*^{ash} male mice aged 5–8 weeks that were genotyped as described previously.[58] For AAV-mediated knockdown of endogenous OTC expression, 5×10^{11} vector genomes of rAAV2/rh10-shRNA-OTC[59] were injected intraperitoneally. Mice were euthanized upon development of signs of hyperammonemia, including ataxia, tremors, and lethargy, which was also documented by the dramatic loss of body weight. All mice were maintained under a 12:12-h dark/light cycle in a standardized environment with controlled humidity and temperature. Mice were offered *ad libitum* standard chow and water.

Surgical intervention in mice

For pain relief, mice received a combination of 0.1 mg/kg buprenorphine (Temgesic; Indivior Schweiz, Baar, Switzerland) and 5 mg/kg carprofen (Rimadyl; Pfizer, New York, NY, USA) subcutaneously 30 min before surgery. Mice were anesthetized in an enclosed container with isoflurane (5% vehicled by oxygen 1 L/min); thereafter, the isoflurane mask was fixed over the nose with continuous treatment of 2%–3% isoflurane vehicled by oxygen 1 L/min. Mice were placed on a surgical board on top of a heating pad (37°C). Thereafter, eyes were covered with vitamin A (retinol) for moisturization. The surgical field was shaved with an electric clipper and disinfected with antiseptic povidone-iodine solution (Braunol; B. Braun, Melsungen, Germany). The abdomen was opened through a longitudinal midline incision.

Hydrodynamic retrograde intrabiliary injection

For HRII, the peritoneal cavity was exposed and the liver was freed from its ligaments, besides the falciform ligament which was connected to the gallbladder. The duodenum and intestine were placed

to the left side of the mouse body and wrapped with gauze moistened with saline. The ideal infusion site was on the fundus of the gallbladder. A short silk thread was placed under the body of the gallbladder, and a loose ligature was made. The infusion catheter (Insyte Autoguard, 24GA; BD, Allschwil, Switzerland) was carefully inserted into the gallbladder, the ligature was tightened, and a surgical knot was made to fix the catheter. For pressurized infusion, portal vein, hepatic artery, and common bile duct were clamped by a single non-traumatic microvessel clamp (Fine Science Tools, North Vancouver, Canada). The suprahepatic vena cava was clamped by a bulldog vessel clamp (FE021K; B. Braun) to completely block the inflow and outflow of the liver shortly during infusion. 0.4–1.0 mL of a saline solution (0.9% NaCl; B. Braun) containing different amounts of MC vectors or plus/minus 15% mannitol were injected in 10–30 s into the gallbladder with a programmable electronic infusion pump device (Standard Infuse/Withdraw Pump 11 Elite Programmable Syringe Pump; Harvard Apparatus, Holliston, MA, USA). After infusion, the bulldog vessel clamp that closed the suprahepatic vena cava was immediately removed followed by the removal of the microvessel clamp that closed the hepatic hilar area. The infusion catheter was subsequently carefully withdrawn from the gallbladder. The cystic duct was ligated with an 8-0 suture (Prolene; Ethicon, Edinburgh, UK), and a cholecystectomy was performed. The duodenum and intestine were then placed back into the abdomen. The abdominal wall was closed using a double-layer continuous running suture technique with a 5-0 suture (Prolene; Ethicon).

Autophagy stimulation was performed by pre-treating animals with 20 mg/kg torin 1 (Sleckchem, Houston, TX, USA) by intraperitoneal injection 2 h prior to HRII.

Hydrodynamic tail vein injection

A saline solution (0.9% NaCl; B. Braun) containing MC vectors was injected via the tail vein, as described previously.[19,20] In brief, mice were injected with 10% body weight of a saline solution containing MC vectors with a 27-gauge needle within 5–8 s. Mice received 5 mg/kg carprofen (Pfizer) subcutaneously after successful injection.

Hydrodynamic portal vein injection

For hydrodynamic intraportal vein injection, the intestines were displaced to the left side of the mouse body to expose portal vein and supra- and infrahepatic vena cava, and wrapped with gauze moistened with saline. The suprahepatic vena cava was clamped by a bulldog vessel clamp (FE021K; B. Braun) to completely block the outflow of the liver shortly during infusion. Hypertonic solutions containing 15% mannitol (B. Braun) and 2.5 units/mL of heparin as well as MC vectors were manually injected over approximately 30 s into the portal vein using a 29-gauge needle into the portal vein with a volume of 0.5 mL. The clamp was removed after the injection was completed. The abdomen wall was closed using a double-layer continuous running suture technique with a 5-0 suture (Prolene; Ethicon).

HRII condition comparison

(1) Vector dose

Three different doses of MC.Luc3, i.e., 2.5 μg, 12.5 μg, and 25 μg DNA per gram of mouse, were infused in a volume of 0.8 mL over 10 s (in saline; flow rate 80 μL/s).

(2) Additives

A study by Budker and colleagues reported that gene expression was 10-fold higher when DNA vectors were delivered in a hypertonic solution containing 15% mannitol.[34] A different study by Hösel and colleagues demonstrated that pharmacological inducers of autophagy enhanced transduction efficiency of AAV vectors in hepatocytes,[69] whereby pre-treatment with a single dose of the autophagy inducer torin 1, an inhibitor of mTOR, increased AAV vector-mediated transgene expression of up to 5-fold in mouse liver. We tested both additives separately in our HRII approach, i.e., either vector infusion in a hypotonic solution with 15% mannitol or pre-treatment with 20 mg/kg of torin 1 intraperitoneally 2 h before vector infusion (2.5 μg/g MC.Luc3, 0.8 mL saline in 10 s; flow rate of 80 μL/s).

(3) Flow rates (volume)

Mice were infused in 10 s with 2.5 μg/g MC.Luc3 in volumes of 0.4 mL, 0.6 mL, and 0.8 mL of saline, equivalent to flow rates of 40 μL/s, 60 μL/s, and 80 μL/s, respectively. To include a flow rate of 100 μL/s without further increasing the total volume, we infused 0.5 mL in 5 s.

(4) High-pressure versus low-pressure injection in combination with mannitol

Mice received 2.5 μg/g MC.Luc3 in 15% mannitol in combination with "low-pressure" (40 μL/s) or "high-pressure" (80 μL/s) infusion.

Analysis of minicircle degradation in bile

Bile was collected from the gallbladder of mice, shock frozen in liquid nitrogen, and stored at −80°C. Bile was added to 1 μg of MC.Luc3 diluted in PBS to a final bile concentration of 10% (v/v). The solution was incubated at 37°C. At the time points of 0, 5, 20, 40, 60, 120 min, aliquots were collected and kept on dry ice until analysis by gel electrophoresis on a 0.8% agarose gel. GelRed (Biotium, Hayward, CA, USA) was used for DNA visualization.

In vivo bioimaging system

Mice were anesthetized with 3%–4% of isoflurane in an induction chamber and injected intraperitoneally with 150 mg/kg D-luciferin potassium salt (Gold Biotechnology, St. Louis, MO, USA). Ten minutes after D-luciferin injection, mice were screened for bioluminescence with an *in vivo* bioimaging system (IVIS 200; PerkinElmer, Santa Clara, CA, USA). Bioluminescence was presented in photons/s and quantified by using Living Image 3.2 software (PerkinElmer). The background level of luciferase expression

(1.4×10^5 photons/s) was determined in five mice which received no MC vectors.

Minicircle production

All minicircle (MC)-producer plasmids with the various expression cassettes were constructed according to the description under "MC vector construction," including plasmids pMC.mOTC2, pMC.mOTC3, pMC.mOTC4, pMC.mOTC7, pMC.Luc3, and pMC.PKU37. All vectors contain a synthetic liver-specific promoter, P3,[20,70] and the bovine growth hormone poly(A) signal (BHGpA). After transforming the MC-producer plasmids into *E. coli* ZYCY10P3S2T, corresponding MC vectors were generated and purified by using The NucleoBond Xtra Maxi EF with the NucleoBond Finisher Maxi (Machery-Nagel, Düren, Germany) according to the manufacturer's instructions. MC quality was analyzed by gel electrophoresis and Sanger sequencing.

MC vector construction

In the following, the various expression cassettes are briefly described.

For pMC.mOTC2 and pMC.mOTC3, vectors were generated by excising *mPah*-cDNA from pMC.PKU20[20] using *Nru*I and *Bsi*WI. pMC.mOTC2 consists of a codon-optimized murine *Otc* (*mcoOTC*) while pMC.mOTC3 contains a codon-optimized *mOtc* combined with an insertion of a 670 bp truncated IVIS1D intron fragment, which retains 300 bp from the 5′ end and 370 bp from the 3′ end of *mOtc* IVIS1 but lacks 12 kb from the native intron, between exon 1 and exon 2 in *mOtc* cDNA. Both inserts were synthesized by GenScript (Piscataway, NJ, USA).

For pMC.mOTC4, the mouse *Otc*-cDNA (ENSMUSG00000031173) containing the murine 5′ Kozak consensus sequence was amplified by PCR from plasmid pAM-LSP1-mOTC[59] with primers containing the terminal restriction sites *Nru*I (underlined in forward primer: 5′-AAT CGC GAG AAT TCG CCG CCA CCA TG-3′) and *Pvu*I (underlined in reverse primer: 5′-CCA CGA TCG ATC GAT AAG CTT ATA TC-3′). The amplified *Otc*-cDNA fragment replaced *mcoOTC* between the P3 promoter and the bovine hormone poly(A) (BGHpA) in vector pMC.mOTC2 to obtain pMC.mOTC4.

For pMC.mOTC7, a FLAG-tag sequence (DYKDDDDK), flanked by additional glycine-glycine residues (as flexible spacers) at both ends (Figure S1A), was inserted C-terminal of the OTC leader peptide[71–73] of pMC.mOTC3 with the Q5 Site-Directed Mutagenesis Kit (New England BioLabs, Ipswich, MA, USA) with the primer pair: forward primer 5′-gat gac gac aag ggt ggt CAA GTA CAG CTC AAG GGC-3′ and reverse primer 5′-gtc ttt gta gtc acc acc ACT TTG GAC TGG CTT CCC-3′ (uppercase = target-specific primer; lowercase = FLAG sequence).

pMC.Luc3 was described in our previous publication as MC.P3-luc[74] expressing the firefly luciferase reporter transgene. The size of MC.Luc3 is 2,326 bp.

pMC.PKU37 consists of FLAG-tagged wild-type mouse phenylalanine hydroxylase (*mPah*-cDNA, ENSMUST00000020241), which was described in our previous publications.[19,20] The size of MC.PKU37 is 2,158 bp.

Vector copy number quantification by quantitative real-time PCR

Genomic DNA (gDNA) from powdered liver tissue was extracted using the DNeasy Blood and Tissue Kit (Qiagen, Homebrechtikon, Switzerland) according to the manufacturer's instructions. The vector copy number per diploid genome was determined by quantitative real-time PCR using primers and probes specific to the BGHpA of the MC vector (forward primer: 5′-GCC TTC TAG TTG CCA GCC AT-3′; reverse primer: 5′-GGC ACC TTC CAG GGT CAA G-3′; probe: 5′-FAM-TGT TTG CCC CTC CCC CGT GC-TAMRA-3′). The *Gapdh* Taqman assay (Mm99999915_g1; Thermo Fischer Scientific, Basel, Switzerland) was included as loading control and the BHGpA signal was then normalized to the *Gapdh* signal. One hundred nanograms of gDNA from each sample was used as a template. The reaction conditions were as follows: 50°C for 2 min and 95°C for 10 min, followed by 40 cycles of 95°C for 15 s and 60°C for 1 min. Quantitative PCR reactions were performed by ABI PRISM 7900 sequence detector, and the data were analyzed with Sequence Detection System V2.4.1. The copy number in 100 ng of gDNA for each sample was calculated as described previously.[19,20] A standard curve plotting cycle threshold (Ct; y axis) against log vector copy number (x axis) was generated using serially diluted DNA vector with various copy numbers (2×10^7 copies to 200 copies) along with 100 ng of non-infused control gDNA.

Histological and immunohistochemical analysis

Formalin-fixed paraffin-embedded liver tissues were sectioned (3–5 μm) and either routinely stained with hematoxylin and eosin (H&E) or subjected to immunohistochemical staining for the expression of luciferase, as previously described.[75] Sections were dewaxed, dehydrated, and subjected to antigen retrieval (20 min incubation at 98°C in EDTA buffer [pH 9] in a pressure cooker), followed by incubation with the primary antibody (goat anti-firefly luciferase, ab16466; Abcam, Cambridge, UK) overnight at 4°C. After blocking of endogenous peroxidase (peroxidase block; Dako, Jena, Germany) for 10 min at room temperature, sections were incubated for 30 min at room temperature with the detection system (Envision System HRP Goat; Agilent Technologies, Basel, Switzerland), with diaminobenzidine as chromogen and counterstained with hematoxylin.

Immunohistochemical staining for FLAG tag and Ki-67 was carried out at the Immunohistochemistry (IHC) Laboratory, Department of Visceral and Transplantation Surgery, University Hospital Zürich (Zürich, Switzerland). Antigen retrieval was performed with Target Retrieval Solution low (pH 6.0, for FLAG tag; Agilent Technologies) or Target Retrieval Solution high (pH 9.0, for Ki-67; Agilent Technologies) in the PT Link autostrainer (Agilent Technologies). Sections were incubated with primary antibodies (rabbit polyclonal anti-DYKDDDK-tag [cat. #14793] in 1:800 dilution; Cell Signaling

Technologies, Danvers, MA, USA) or rabbit monoclonal anti-Ki67 (#ab16667) in 1:200 dilution; Abcam) in Dako REAL antibody diluent, followed by Envision System HRP Rabbit (Agilent Technologies).

Sections stained for FLAG tag and Ki-67 were imaged using the Axio Scan.Z1 slide scanner (Zeiss, Oberkochen, Germany) and analyzed using FIJI (2.0.0-rc-43/1.50e, Java 1.6.0_24 [64-bit]) and the ImmunoRatio plugin.[20]

RNA extraction, RNA sequencing, cluster generation, and bioinformatics

The QIamp RNA Blood Mini Kit (Qiagen, Hilden, Germany) was used for RNA extraction of homogenized mouse liver according to the manufacturer's instructions. The tissue protocol was used with the optional a DNase digestion step. The quality of the isolated RNA was determined with a Qubit (1.0) Fluorometer (Life Technologies, Carlsbad, CA, USA) and a Fragment Analyzer (Agilent, Santa Clara CA, USA). Only those samples with a 260 nm/280 nm ratio between 1.8 and 2.1 and a 28S/18S ratio within 1.5–2 were further processed. The TruSeq Stranded mRNA (Illumina, San Diego, CA, USA) was used in the succeeding steps. In brief, 500 ng of total RNA samples were poly(A) enriched and then reverse transcribed into double-stranded cDNA. The cDNA samples were fragmented, end-repaired, and adenylated before ligation of TruSeq adapters containing unique dual indices for multiplexing. Fragments containing TruSeq adapters on both ends were selectively enriched with PCR. The quality and quantity of the enriched libraries were validated using a Qubit (1.0) Fluorometer and the Fragment Analyzer (Agilent). The product is a smear with an average fragment size of approximately 260 bp. The libraries were normalized to 10 nM in 10 mM Tris-Cl, pH 8.5 with 0.1% Tween 20. The Novaseq 6000 (Illumina) was used for cluster generation and sequencing according to standard protocol. The sequencing mode was paired end at 2 × 150 bp or single end at 100 bp.

The raw reads were first cleaned by removing adapter sequences, trimming low-quality ends, and filtering reads with low quality (phred quality <20) using Trimmomatic (version 0.36). Sequence pseudo-alignment of the resulting high-quality reads to the mouse reference genome (build GRCm38.p5) and quantification of gene level expression were carried out using Kallisto (version 0.44).[76]

DEGs were identified by the R package edgeR (v3.26.1) using a generalized linear model (glm) regression, a quasi-likelihood differential expression test, and the trimmed means of M-values normalization. Genes showing altered expression with adjusted (Benjamini and Hochberg method) p value <0.05 and $\log_2$(fold change) >0.5 were considered differentially expressed.[77]

Ureagenesis assay

Quantification of ureagenesis was followed as described in our published protocol.[58] In brief, mice were fasted for 3–4 h. Duplicates of basal blood sample (5 μL) before tracer injection were collected on a filter card (IDBS-226; PerkinElmer, Shelton, CT, USA) by tail vein puncture. Thereafter, mice received [15N]H_4Cl tracer (4 mmol/kg body weight, dissolved in 1× PBS) intraperitoneally. Following 30 min, new duplicates (5 μL) were collected. Samples were prepared, and enrichment of [15N]H_4Cl was measured according to Allegri et al.[58]

AAV vector production

The vector constructs for knockdown of endogenous OTC mRNA and rAAV2/rh10 were produced as described previously.[59,78]

Ornithine transcarbamylase assay

The OTC enzyme assay from liver lysate was performed as previously described.[58] In brief, an assay mixture containing triethanolamine (270 mM), ornithine (5 mM), and carbamoyl phosphate (15 mM) was prepared and 5 μL of liver lysate, equivalent to 0.5–15 μg of total protein, was added. The reaction mixture was incubated at 37°C for 30 min and stopped with 3:1 phosphoric acid/sulfuric acid (v/v). Citrulline production was determined with 3% 2,3-butanedione monoxime, by incubating at 95°C–100°C in darkness for 15 min. Absorbance was measured at 490 nm (Ultrospec 3100 Pro; Amersham Biosciences, Amersham, UK).

Collection of liver and other organ samples

Animals were perfused with heparinized 1× DPBS (Heparin-Na; B. Braun) through the left cardiac chamber using a peristaltic pump (P-1 Peristaltic Pump; Amersham Biosciences). Outflow was ensured by cutting the vena cava. Other organs such as brain, kidney, pancreas, stomach, and duodenum were dissected and snap-frozen in liquid nitrogen. One piece of each liver lobe was collected according to Figure S6, stored in a 4% formaldehyde solution (pH 6.9) (Merck, Darmstadt, Germany) for 24 h, and subsequently transferred to 70% ethanol (Merck) at 4°C for 3–4 days, then trimmed and routinely paraffin-wax embedded for the histological examination. Frozen tissues were kept at −80°C.

Analysis of MC vector by saturated PCR

Liver tissue was homogenized using the Tissue-Lyser II (Qiagen, Hombrechtikon, Switzerland). DNA was extracted from liver homogenates using the DNeasy Blood and Tissue Kit (Qiagen) according to the manufacturer's protocol. Purity and quality of DNA were measured with NanoDrop ND1000 (Thermo Fisher Scientific). PCR with DNA isolated from the tissue samples was performed to determine presence of MC vectors. Primer f2 luc 5′-CAC GTT CGT CAC ATC TCA TCT ACC-3′ and reverse primer r3 luc 5′-TGA GCC CAT ATC CTT GCC TGA TAC-3′ were obtained to amplify the luciferase transgene. PCR for 42 cycles using HOT FIREPol polymerase (Solis BioDyne, Luzerne, Switzerland) was performed at an annealing temperature of 58°C. The amplified fragment had an expected length of 533 bp.

Luciferase enzyme assay

The Luciferase Assay System (Promega, Dübendorf, Switzerland) on the microplate reader infinite F200 (Tecan, Männedorf, Switzerland) was used to determine the luciferase activity according to the

manufacturer's protocol. Tecan i-control 1.10 software was used for data analysis. The threshold hold of the luciferase enzyme activity was defined as 0.08 RLU/μg protein, which was measured in five mice which received no MC vectors.

Liver enzyme and blood ammonia diagnostics

Blood was collected immediately after euthanization with CO_2 and transferred into Li-heparin tubes (Microvette 200; Sarstedt, Newton, NC, USA). Tubes were centrifuged at 2,000 × *g* for 10 min. Plasma was transferred into an Eppendorf tube, snap-frozen in liquid nitrogen, and kept at −80°C. Plasma (minimum 50 μL) biochemical analyses were done by the Division of Clinical Chemistry and Biochemistry at the University Children's Hospital Zürich (Zürich, Switzerland) with a commercial routine method on an Alinity c (Abbot Laboratories, Chicago, IL, USA).

Immunofluorescence

Formalin-fixed paraffin-embedded liver tissues were sectioned and stained for FLAG tag and HSP60 at IHC Laboratory of the Center for Surgical Research at the University Hospital Zürich. Sections were treated as follows. Antigen retrieval was performed with Target Retrieval Solution low (pH 6.0) in the PT Link (Dako, Glostrup, Denmark). Autofluorescence was quenched with TrueBlack (23007; Biotium, Hayward, CA, USA) according to the manufacturer's instructions. Sections were incubated with anti-FLAG (1:800, diluted in DAKO REAL antibody diluent, cat. #14793; Cell Signaling), washed and incubated with Alexa Green 488 (2 μg/mL, A21206; Thermo Fisher Scientific), or incubated with anti-HSP60 (1:100, diluted in DAKO REAL antibody diluent, ab109873; Abcam), washed and incubated with Alexa Red 594 (2 μg/mL, A 11058; Thermo Fisher Scientific). Finally, slides were mounted with DAPI mounting medium (1 drop, ab104139; Abcam). The images were acquired with a Leica SP8 confocal microscope at the Center of Microscopy and Image Analysis at the University of Zürich. The images were deconvoluted with Huygens (version 19.4), and the co-localization analysis was performed with Imaris (version 9.3).

Western blotting

Proteins were detected by SDS-PAGE (Mini-PROTEAN precast gels, 4%–15%; Bio-Rad, Hercules, CA, USA) using antibodies diluted in 5% milk in TBST: anti-goat-DYKDDDDK tag (1:1,000, #14793; Cell Signaling), anti-OTC (1:1,000, ab203859; Abcam), and mouse-anti-β-actin (1:4,000, ab8227; Abcam). Secondary antibodies were conjugated to horseradish peroxidase for visualization in 5% milk in TBST in a 1:3,000 dilution. Chemiluminescence and total protein were recorded with a ChemieDoc Touch Imaging System (Bio-Rad).

Cytokine IL-6 measurement

IL-6 measurement was performed according to the protocol from the manufacturer. In brief, IL-6 was detected with a bead-based immunoassay using fluorescence-encoded beads (LEGENDplex; BioLegend, San Diego, CA, USA). The fluorescent signals were detected by a flow cytometry FACSCanto II (BD Biosciences, Allschwil, Switzerland).

Statistics

Statistical analysis was performed using Prism 8 (version 8.3.1). Continuous variables are reported as mean ± SD unless indicated otherwise. Two-sample comparisons were performed using the two-tailed Student's t test, and multiple comparisons were performed by one-way or two-way ANOVA. The Mann-Whitney U test and Kruskal-Wallis test were used to compare data with a non-normal distribution. Statistical significance is indicated in figures as $^{*}p < 0.05$, $^{**}p < 0.01$, $^{***}p < 0.001$, $^{****}p < 0.0001$, and n.s. ($p > 0.05$).

DATA AVAILABILITY

All data-supporting materials are available within the article and supplemental information.

SUPPLEMENTAL INFORMATION

Supplemental information can be found online at https://doi.org/10.1016/j.omtm.2022.10.006.

ACKNOWLEDGMENTS

We thank Dr. Charles P. Venditti for his suggestions on designing the FLAG-tagged OTC, Ms. Ines Kleiber-Schaaf from the Department of Visceral and Transplantation Surgery, University Hospital Zürich for performing immunofluorescence staining, the Division of Clinical Chemistry and Biochemistry, University Children's Hospital Zürich for routine parameter analyses, the Center for Microscopy and Image Analysis, University of Zürich for the imaging, and the Histology Laboratory, Institute of Veterinary Pathology, Vetsuisse Faculty, University of Zürich for tissue staining. This work was supported by the Swiss National Science Foundation (310030_162547 and CRSII5_180257 to B.T., and 320030_176088 to J.H.), the Rare Disease Initiative Zürich (radiz) of the University of Zürich, the Wolfermann-Nägeli Foundation, the Foundation for Research in Science and the Humanities at the University of Zürich (STWF-18-013 to B.T.), and FZK Heidi-Ras grant (to H.M.G.-C.).

AUTHOR CONTRIBUTIONS

S.D., A.S., Z.S., G.A., N.R., T.S., M.W., L.O., S.C.C., A.K., and H.M.G.-C. performed experiments and analyzed data. S.D., G.A., N.R., T.S., M.W., L.O., S.C.C., I.E.A., A.K., J.H., B.T., and H.M.G.-C., contributed with analyses and/or tools. S.D., B.T., and H.M.G.-C. conceived and managed the project. B.T. and H.M.G.-C. wrote the manuscript with the contribution of all authors. All authors read and approved the manuscript. B.T. and H.M.G.-C. are co-correspondent authors.

DECLARATION OF INTERESTS

The authors declare no competing interests.

REFERENCES

1. Dunbar, C.E., High, K.A., Joung, J.K., Kohn, D.B., Ozawa, K., and Sadelain, M. (2018). Gene therapy comes of age. Science *359*. eaan4672.

2. Maestro, S., Weber, N.D., Zabaleta, N., Aldabe, R., and Gonzalez-Aseguinolaza, G. (2021). Novel vectors and approaches for gene therapy in liver diseases. JHEP Reports *3*, 100300.

3. Dalwadi, D.A., Calabria, A., Tiyaboonchai, A., and Posey, J., Naugler, W.E., Montini, E., and Grompe, M.. (2021). AAV integration in human hepatocytes. Mol. Ther. *29*, 2898–2909.
4. Colella, P., Ronzitti, G., and Mingozzi, F.. (2018). Emerging issues in AAV-mediated in vivo gene therapy. Mol. Ther. Methods Clin. Dev. *8*, 87–104.
5. Dalwadi, D.A., Torrens, L., Abril-Fornaguera, J., Pinyol, R., Willoughby, C., Posey, J., Llovet, J.M., Lanciault, C., Russell, D.W., Grompe, M., et al.. (2021). Liver injury increases the incidence of HCC following AAV gene therapy in mice. Mol. Ther. *29*, 680–690.
6. Venditti, C.P.. (2021). Safety questions for AAV gene therapy. Nat. Biotechnol. *39*, 24–26.
7. Keiser, M.S., Ranum, P.T., Yrigollen, C.M., Carrell, E.M., Smith, G.R., Muehlmatt, A.L., Chen, Y.H., Stein, J.M., Wolf, R.L., Radaelli, E., et al. (2021). Toxicity after AAV delivery of RNAi expression constructs into nonhuman primate brain. Nat. Med. *27*, 1982–1989.
8. Monahan, P.E., Négrier, C., Tarantino, M., Valentino, L.A., and Mingozzi, F. (2021). Emerging immunogenicity and genotoxicity considerations of adeno-associated virus vector gene therapy for hemophilia. J. Clin. Med. *10*, 2471.
9. Witzigmann, D., Kulkarni, J.A., Leung, J., Chen, S., Cullis, P.R., and van der Meel, R. (2020). Lipid nanoparticle technology for therapeutic gene regulation in the liver. Adv. Drug Deliv. Rev. *159*, 344–363.
10. Hardee, C., Arévalo-Soliz, L., Hornstein, B., and Zechiedrich, L. (2017). Advances in non-viral DNA vectors for gene therapy. Genes *8*, 65.
11. Kulkarni, J.A., Witzigmann, D., Thomson, S.B., Chen, S., Leavitt, B.R., Cullis, P.R., and van der Meel, R. (2021). The current landscape of nucleic acid therapeutics. Nat. Nanotechnol. *16*, 630–643.
12. Gaspar, V., de Melo-Diogo, D., Costa, E., Moreira, A., Queiroz, J., Pichon, C., Correia, I., and Sousa, F. (2015). Minicircle DNA vectors for gene therapy: advances and applications. Expert Opin. Biol. Ther. *15*, 353–379.
13. Luke, J.M., Carnes, A.E., and Williams, J.A. (2014). Development of antibiotic-free selection system for safer DNA vaccination. Methods Mol. Biol. *1143*, 91–111.
14. Quiviger, M., Arfi, A., Mansard, D., Delacotte, L., Pastor, M., Scherman, D., and Marie, C. (2014). High and prolonged sulfamidase secretion by the liver of MPS-IIIA mice following hydrodynamic tail vein delivery of antibiotic-free pFAR4 plasmid vector. Gene Ther. *21*, 1001–1007.
15. Liu, F., Song, Y., and Liu, D. (1999). Hydrodynamics-based transfection in animals by systemic administration of plasmid DNA. Gene Ther. *6*, 1258–1266.
16. Zhang, G., Budker, V., and Wolff, J.A. (1999). High levels of foreign gene expression in hepatocytes after tail vein injections of naked plasmid DNA. Hum. Gene Ther. *10*, 1735–1737.
17. Bonamassa, B., Hai, L., and Liu, D. (2011). Hydrodynamic gene delivery and its applications in pharmaceutical research. Pharm. Res. (N. Y.) *28*, 694–701.
18. Dalsgaard, T., Cecchi, C.R., Askou, A.L., Bak, R.O., Andersen, P.O., Hougaard, D., Jensen, T.G., Dagnæs-Hansen, F., Mikkelsen, J.G., Corydon, T.J., and Aagaard, L. (2018). Improved lentiviral gene delivery to mouse liver by hydrodynamic vector injection through tail vein. Mol. Ther. Nucleic Acids *12*, 672–683.
19. Grisch-Chan, H.M., Schlegel, A., Scherer, T., Allegri, G., Heidelberger, R., Tsikrika, P., Schmeer, M., Schleef, M., Harding, C.O., Häberle, J., and Thöny, B. (2017). Low-dose gene therapy for murine PKU using episomal naked DNA vectors expressing PAH from its endogenous liver promoter. Mol. Ther. Nucleic Acids *7*, 339–349.
20. Viecelli, H.M., Harbottle, R.P., Wong, S.P., Schlegel, A., Chuah, M.K., VandenDriessche, T., Harding, C.O., and Thöny, B. (2014). Treatment of phenylketonuria using minicircle-based naked-DNA gene transfer to murine liver. Hepatology *60*, 1035–1043.
21. Lee, H.O., Gallego-Villar, L., Grisch-Chan, H.M., Häberle, J., Thöny, B., and Kruger, W.D. (2019). Treatment of cystathionine β-synthase deficiency in mice using a minicircle-based naked DNA vector. Hum. Gene Ther. *30*, 1093–1100.
22. Summar, M.L., Koelker, S., Freedenberg, D., Le Mons, C., Haberle, J., Lee, H.S., and Kirmse, B.; European Registry and Network for Intoxication Type Metabolic Diseases E-IMD. Electronic address: http://www.e-imd.org/en/index.phtml; Members of the Urea Cycle Disorders Consortium UCDC. Electronic address: http://rarediseasesnetwork.epi.usf.edu/ucdc/ (2013). The incidence of urea cycle disorders. Mol. Genet. Metab. *110*, 179–180.
23. Ah Mew, N., Simpson, K.L., Gropman, A.L., Lanpher, B.C., Chapman, K.A., and Summar, M.L. (1993). Urea Cycle Disorders Overview.
24. Häberle, J., Burlina, A., Chakrapani, A., Dixon, M., Karall, D., Lindner, M., Mandel, H., Martinelli, D., Pintos-Morell, G., Santer, R., et al. (2019). Suggested guidelines for the diagnosis and management of urea cycle disorders: first revision. J. Inherit. Metab. Dis. *42*, 1192–1230.
25. Yu, L., Rayhill, S.C., Hsu, E.K., and Landis, C.S. (2015). Liver transplantation for urea cycle disorders: analysis of the united network for organ sharing database. Transplant. Proc. *47*, 2413–2418.
26. Viecelli, H.M., and Thöny, B. (2014). Challenges of experimental gene therapy for urea cycle disorders. J. Pediatr. Biochem. *4*, 65–73.
27. Wang, L., Bell, P., Morizono, H., He, Z., Pumbo, E., Yu, H., White, J., Batshaw, M.L., and Wilson, J.M. (2017). AAV gene therapy corrects OTC deficiency and prevents liver fibrosis in aged OTC-knock out heterozygous mice. Mol. Genet. Metab. *120*, 299–305.
28. De Sabbata, G., Boisgerault, F., Guarnaccia, C., Iaconcig, A., Bortolussi, G., Collaud, F., Ronzitti, G., Sola, M.S., Vidal, P., Rouillon, J., et al. (2021). Long-term correction of ornithine transcarbamylase deficiency in Spf-Ash mice with a translationally optimized AAV vector. Mol. Ther. Methods Clin. Dev. *20*, 169–180.
29. Ultragenyx Pharmaceutical. (2020). Press Release. Ultragenyx announces positive longer-term results from first three cohorts of phase 1/2 study of DTX301 gene therapy in ornithine transcarbamylase (OTC) deficiency.
30. Agarwal, S. (2020). High-dose AAV gene therapy deaths. Nat. Biotechnol. *38*, 910.
31. Wilson, J.M., and Flotte, T.R. (2020). Moving forward after two deaths in a gene therapy trial of myotubular myopathy. Hum. Gene Ther. *31*, 695–696.
32. Gebhardt, R., and Matz-Soja, M. (2014). Liver zonation: novel aspects of its regulation and its impact on homeostasis. World J. Gastroenterol. *20*, 8491–8504.
33. Morris, S.M. (2002). Regulation of enzymes of the urea cycle and arginine metabolism. Annu. Rev. Nutr. *22*, 87–105.
34. Budker, V., Zhang, G., Knechtle, S., and Wolff, J.A. (1996). Naked DNA delivered intraportally expresses efficiently in hepatocytes. Gene Ther. *3*, 593–598.
35. Braet, F., and Wisse, E. (2002). Structural and functional aspects of liver sinusoidal endothelial cell fenestrae: a review. Comp. Hepatol. *1*, 1–17.
36. Poisson, J., Lemoinne, S., Boulanger, C., Durand, F., Moreau, R., Valla, D., and Rautou, P.E. (2017). Liver sinusoidal endothelial cells: physiology and role in liver diseases. J. Hepatol. *66*, 212–227.
37. Ajiki, T., Onoyama, H., Yamamoto, M., Fujimori, T., Maeda, S., and Saitoh, Y. (1995). Detection of point mutations in K-ras gene at codon 12 in bile from percutaneous transhepatic choledochal drainage tubes for diagnosis of biliary strictures. Int. J. Pancreatol. *18*, 215–220.
38. Zhang, G., Vargo, D., Budker, V., Armstrong, N., Knechtle, S., and Wolff, J.A. (1997). Expression of naked plasmid DNA injected into the afferent and efferent vessels of rodent and dog livers. Hum. Gene Ther. *8*, 1763–1772.
39. Zhang, X., Collins, L., Sawyer, G.J., Dong, X., Qiu, Y., and Fabre, J.W. (2001). In vivo gene delivery via portal vein and bile duct to individual lobes of the rat liver using a polylysine-based nonviral DNA vector in combination with chloroquine. Hum. Gene Ther. *12*, 2179–2190.
40. Poussin, D., Malassagne, B., Tran Van Nhieu, J., Trébéden, H., Guéry, L., Chéreau, C., Soubrane, O., Calmus, Y., Weill, B., and Batteux, F. (2002). Biliary administration of naked DNA encoding Fas-Fc protein prevents acute liver failure in mice. Hum. Gene Ther. *13*, 901–908.
41. Hu, J., Zhang, X., Dong, X., Collins, L., Sawyer, G.J., and Fabre, J.W. (2005). A remarkable permeability of canalicular tight junctions might facilitate retrograde, non-viral gene delivery to the liver via the bile duct. Gut *54*, 1473–1479.
42. Jiang, X., Ren, Y., Williford, J.-M., Li, Z., and Mao, H.-Q. (2013). Liver-targeted gene delivery through retrograde intrabiliary infusion. In Nanotechnology for Nucleic Acid Delivery: Methods and Protocols, M. Ogris and D. Oupicky, eds. (Humana Press), pp. 275–284.

43. Jiang, X., Dai, H., Ke, C.Y., Mo, X., Torbenson, M.S., Li, Z., and Mao, H.Q. (2007). PEG-b-PPA/DNA micelles improve transgene expression in rat liver through intrabiliary infusion. J. Control. Release *122*, 297–304.

44. Kumbhari, V., Li, L., Piontek, K., Ishida, M., Fu, R., Khalil, B., Garrett, C.M., Liapi, E., Kalloo, A.N., and Selaru, F.M. (2018). Successful liver-directed gene delivery by ERCP-guided hydrodynamic injection (with videos). Gastrointest. Endosc. *88*, 755–763.e5.

45. Otsuka, M., Baru, M., Delrivière, L., Talpe, S., Nur, I., and Gianello, P. (2000). In vivo liver-directed gene transfer in rats and pigs with large anionic multilamellar liposomes: routes of Administration and effects of surgical manipulations on transfection efficiency. J. Drug Target. *8*, 267–279.

46. Huang, Y., Kruse, R.L., Ding, H., Itani, M.I., Morrison, J., Wang, Z.Z., Selaru, F.M., and Kumbhari, V. (2021). Parameters of biliary hydrodynamic injection during endoscopic retrograde cholangio-pancreatography in pigs for applications in gene delivery. PLoS One *16*, e0249931.

47. Chan, T., Grisch-Chan, H.M., Schmierer, P., Subotic, U., Rimann, N., Scherer, T., Hetzel, U., Bozza, M., Harbottle, R., Williams, J.A., et al. (2022). Delivery of non-viral naked DNA vectors to liver in small weaned pigs by hydrodynamic retrograde intrabiliary injection. Mol. Ther. Methods Clin. Dev. *24*, 268–279.

48. Valencik, M.L., and McDonald, J.A. (2001). Codon optimization markedly improves doxycycline regulated gene expression in the mouse heart. Transgenic Res. *10*, 269–275.

49. Kuriyama, S., Yoshiji, H., Nakai, S., Deguchi, A., Uchida, N., Kimura, Y., Inoue, H., Kinekawa, F., Ogawa, M., Nonomura, T., et al. (2005). Adenovirus-mediated gene transfer into rat livers: comparative study of retrograde intrabiliary and antegrade intraportal administration. Oncol. Rep. *13*, 69–74.

50. Kuhel, D.G., Zheng, S., Tso, P., and Hui, D.Y. (2000). Adenovirus-mediated human pancreatic lipase gene transfer to rat bile: gene therapy of fat malabsorption. Am. J. Physiol. Gastrointest. Liver Physiol. *279*, G1031–G1036. https://doi.org/10.1152/ajpgi.2000.279.5.g1031.

51. Sullivan, D.E., Dash, S., Du, H., Hiramatsu, N., Aydin, F., Kolls, J., Blanchard, J., Baskin, G., and Gerber, M.A. (1997). Liver-directed gene transfer in non-human primates. Hum. Gene Ther. *8*, 1195–1206.

52. De Godoy, J.L., Malafosse, R., Fabre, M., Mehtali, M., Houssin, D., and Soubrane, O. (1999). In vivo hepatocyte retrovirus-mediated gene transfer through the rat biliary tract. Hum. Gene Ther. *10*, 249–257.

53. Cabrera, J.A., Wilson, J.M., and Raper, S.E. (1996). Targeted retroviral gene transfer into the rat biliary tract. Somat. Cell Mol. Genet. *22*, 21–29.

54. Podevin, G., Ferry, N., Calise, D., and Révillion, Y. (1996). In vivo retroviral-mediated transfer of a marker-gene in ornithine transcarbamylase-deficient Spf(ash) mice. J. Pediatr. Surg. *31*, 1516–1519.

55. Masamune, K., Kunitomo, K., Sasaki, K., Yagi, K., Komi, N., and Tashiro, S. (1997). Bile-induced DNA strand breaks and biochemical analysis of bile acids in an experimental model of anomalous arrangement of the pancreaticobiliary ducts. J. Med. Invest. *44*, 47–51.

56. Wiener, S.M., Hoyt, R.F., Jr., Deleonardis, J.R., Clevenger, R.R., Jeffries, K.R., Nagashima, K., Mandel, M., Owens, J., Eckhaus, M., Lutz, R.J., and Safer, B. (2000). Manometric changes during retrograde biliary infusion in mice. Am. J. Physiol. Gastrointest. Liver Physiol. *279*, G49–G66.

57. Berntsen, N.L., Fosby, B., Valestrand, L., Tan, C., Reims, H.M., Schrumpf, E., Karlsen, T.H., Line, P.D., and Melum, E. (2018). Establishment of a surgical bile duct injection technique giving direct access to the bile ducts for studies of the murine biliary tree. Am. J. Physiol. Gastrointest. Liver Physiol. *314*, G349–G359.

58. Allegri, G., Deplazes, S., Grisch-Chan, H.M., Mathis, D., Fingerhut, R., Häberle, J., and Thöny, B. (2017). A simple dried blood spot-method for in vivo measurement of ureagenesis by gas chromatography-mass spectrometry using stable isotopes. Clin. Chim. Acta *464*, 236–243.

59. Cunningham, S.C., Kok, C.Y., Dane, A.P., Carpenter, K., Kizana, E., Kuchel, P.W., and Alexander, I.E. (2011). Induction and prevention of severe hyperammonemia in the spf ash mouse model of ornithine transcarbamylase deficiency using shRNA and rAAV-mediated gene delivery. Mol. Ther. *19*, 854–859.

60. Hadjantonakis, A.K., Dickinson, M.E., Fraser, S.E., and Papaioannou, V.E. (2003). Technicolour transgenics: imaging tools for functional genomics in the mouse. Nat. Rev. Genet. *4*, 613–625.

61. Podetz-Pedersen, K.M., Vezys, V., Somia, N.V., Russell, S.J., and McIvor, R.S. (2014). Cellular immune response against firefly luciferase after sleeping beauty-mediated gene transfer in vivo. Hum. Gene Ther. *25*, 955–965.

62. Lu, J., Zhang, F., and Kay, M.A. (2013). A mini-intronic plasmid (MIP): a novel robust transgene expression vector in vivo and in vitro. Mol. Ther. *21*, 954–963.

63. Limberis, M.P., Bell, C.L., and Wilson, J.M. (2009). Identification of the murine firefly luciferase-specific CD8 T-cell epitopes. Gene Ther. *16*, 441–447.

64. Jeon, Y.H., Choi, Y., Kang, J.H., Kim, C.W., Jeong, J.M., Lee, D.S., and Chung, J.K. (2007). Immune response to firefly luciferase as a naked DNA. Cancer Biol. Ther. *6*, 781–786.

65. Grompe, M., and Strom, S. (2013). Mice with human livers. Gastroenterology *145*, 1209–1214.

66. Nygaard, S., Barzel, A., Haft, A., Major, A., Finegold, M., Kay, M.A., and Grompe, M. (2016). A universal system to select gene-modified hepatocytes in vivo. Sci. Transl. Med. *8*, 342ra79.

67. Vonada, A., Tiyaboonchai, A., Nygaard, S., Posey, J., Peters, A.M., Winn, S.R., Cantore, A., Naldini, L., Harding, C.O., and Grompe, M. (2021). Therapeutic liver repopulation by transient acetaminophen selection of gene-modified hepatocytes. Sci. Transl. Med. *13*, eabg3047.

68. Bozza, M., De Roia, A., Correia, M.P., Berger, A., Tuch, A., Schmidt, A., Zörnig, I., Jäger, D., Schmidt, P., and Harbottle, R.P. (2021). A nonviral, nonintegrating DNA nanovector platform for the safe, rapid, and persistent manufacture of recombinant T cells. Sci. Adv. *7*, eabf1333.

69. Hösel, M., Huber, A., Bohlen, S., Lucifora, J., Ronzitti, G., Puzzo, F., Boisgerault, F., Hacker, U.T., Kwanten, W.J., Klöting, N., et al. (2017). Autophagy determines efficiency of liver-directed gene therapy with adeno-associated viral vectors. Hepatology *66*, 252–265.

70. Nair, N., Rincon, M.Y., Evens, H., Sarcar, S., Dastidar, S., Samara-Kuko, E., Ghandeharian, O., Man Viecelli, H., Thöny, B., De Bleser, P., et al. (2014). Computationally designed liver-specific transcriptional modules and hyperactive factor IX improve hepatic gene therapy. Blood *123*, 3195–3199.

71. Sztul, E.S., Hendrick, J.P., Kraus, J.P., Wall, D., Kalousek, F., and Rosenberg, L.E. (1987). Import of rat ornithine transcarbamylase precursor into mitochondria: two-step processing of the leader peptide. J. Cell Biol. *105*, 2631–2639.

72. Gakh, O., Cavadini, P., and Isaya, G. (2002). Mitochondrial processing peptidases. Biochim. Biophys. Acta *1592*, 63–77.

73. Isaya, G., Kalousek, F., Fenton, W.A., and Rosenberg, L.E. (1991). Cleavage of precursors by the mitochondrial processing peptidase requires a compatible mature protein or an intermediate octapeptide. J. Cell Biol. *113*, 65–76.

74. Stoller, F., Schlegel, A., Viecelli, H.M., Rüfenacht, V., Cesarovic, N., Viecelli, C., Deplazes, S., Bettschart, R., Hurter, K., Schmierer, P., et al. (2015). Hepatocyte transfection in small pigs after weaning by hydrodynamic intraportal injection of naked DNA/minicircle vectors. Hum. Gene Ther. Methods *26*, 181–192.

75. Forootan, S.S., Mutter, F.E., Kipar, A., Iwawaki, T., Francis, B., Goldring, C.E., Park, B.K., and Copple, I.M. (2017). Real-time in vivo imaging reveals localised Nrf2 stress responses associated with direct and metabolism-dependent drug toxicity. Sci. Rep. *7*, 16084.

76. Bolger, A.M., Lohse, M., and Usadel, B. (2014). Trimmomatic: a flexible trimmer for Illumina sequence data. Bioinformatics *30*, 2114–2120.

77. Bray, N.L., Pimentel, H., Melsted, P., and Pachter, L. (2016). Near-optimal probabilistic RNA-seq quantification. Nat. Biotechnol. *34*, 525–527.

78. Cunningham, S.C., Siew, S.M., Hallwirth, C.V., Bolitho, C., Sasaki, N., Garg, G., Michael, I.P., Hetherington, N.A., Carpenter, K., de Alencastro, G., et al. (2015). Modeling correction of severe urea cycle defects in the growing murine liver using a hybrid recombinant adeno-associated virus/piggyBac transposase gene delivery system. Hepatology *62*, 417–428.